

¹

Observation of a Critical Charge Mode in a Strange Metal

²

³ Hisao Kobayashi,^{1,2*} Yui Sakaguchi,¹ Hayato Kitagawa,^{1,2} Momoko Oura,^{1,2}
Shugo Ikeda,^{1,2} Kentaro Kuga,³ Shintaro Suzuki,³ Satoru Nakatsuji,^{3,4,5,6*}
Ryo Masuda,^{2,7,8} Yasuhiro Kobayashi,^{2,7} Makoto Seto,^{2,7}
Yoshitaka Yoda,⁹ Kenji Tamasaku,²
Yashar Komijani,^{10,11} Premala Chandra,¹¹ Piers Coleman^{11,12*}

¹Graduate School of Material Science, University of Hyogo, 3-2-1 Koto, Hyogo 678-1297, Japan

²RIKEN SPring-8 Center, Hyogo 679-5148, Japan

³Institute for Solid State Physics, University of Tokyo, Kashiwa 277-8581, Japan

⁴Department of Physics, University of Tokyo, Hongo, Bunkyo-ku, Tokyo 113-0033, Japan

⁵Trans-scale Quantum Science Institute, University of Tokyo, Bunkyo-ku, Tokyo 113-0033, Japan

⁶Institute for Quantum Matter and Department of Physics and Astronomy,
Johns Hopkins University, Baltimore, Maryland 21218, USA

⁷Institute for Integrated Radiation and Nuclear Science, Kyoto University, Osaka 590-0494, Japan

⁸Graduate School of Science and Technology, Hirosaki University, Aomori 036-8561 Japan

⁹Japan Synchrotron Radiation Research Institute, Hyogo 679-5198, Japan

¹⁰Department of Physics, University of Cincinnati, Cincinnati, Ohio 45221-0011, USA

¹¹Department of Physics and Astronomy, Rutgers University, Piscataway, New Jersey 08854, USA

¹²Hubbard Theory Consortium, Department of Physics,
Royal Holloway, University of London, Egham, Surrey TW20 0EX, UK

*To whom correspondence should be addressed; E-mail: kobayash@sci.u-hyogo.ac.jp,
satoru@phys.s.u-tokyo.ac.jp, coleman@physics.rutgers.edu

⁴October 10, 2022

5 **Quantum electronic matter has long been understood in terms of two limiting**
6 **behaviors of electrons: one of delocalized metallic states, and the other of lo-**
7 **calized magnetic states. Understanding the strange metallic behavior which**
8 **develops at the brink of localization demands new probes of the underlying**
9 **electronic charge dynamics. Using a state-of-the-art technique, synchrotron-**
10 **radiation-based Mössbauer spectroscopy, we have studied the longitudinal charge**
11 **fluctuations of the strange metal phase of β -YbAlB₄ as a function of tempera-**
12 **ture and pressure. We find that the usual single absorption peak in the Fermi-**
13 **liquid regime splits into two peaks upon entering the critical regime. This**
14 **spectrum is naturally interpreted as a single nuclear transition, modulated by**
15 **nearby electronic valence fluctuations whose long time-scales are further en-**
16 **hanced, due to the formation of charged polarons. Our results represent a**
17 **direct observation of critical charge fluctuations as a new signature of strange**
18 **metals.**

19 The strange metal (SM) is a ubiquitous state of matter found to develop in quantum materials
20 with strong correlations, often appearing as a fan-shaped region of the phase diagram centered
21 around an unstable quantum critical (QC) point. SMs share many commonalities, most-notably
22 a logarithmic temperature (T) dependence of specific heat $C/T \sim -\log T$, a linear-in- T re-
23 sistivity $\rho(T) \sim T$ (1) and a strong violation of Kohlers law in the magnetotransport (2, 3, 4).
24 These properties and their universality defy the standard concept of quasiparticle excitations
25 and the conventional wisdom of momentum-relaxation-origin of the conductivity, central to the
26 Fermi liquid (FL) theory of metals. This enigma has prompted a wide range of possible ori-
27 gins, including spin-density instability (1), Fermi surface instability (5, 6, 7), valence quantum
28 criticality (8), charge stripes (9), and nematicity (10, 11, 12) and motivated novel approaches,
29 including the holographic duality (13, 14, 15) and simulation using cold atoms (16).

30 While the spin dynamics at quantum criticality has been extensively studied, little is known
31 experimentally about the charge dynamics as appropriate laboratory probes are scarce. Conven-
32 tionally, charge dynamics are studied using optical spectroscopy (17), but these methods only
33 probe the low-momenta, divergence-free *transverse* components of the current $\mathbf{J} = \sigma \mathbf{E} \perp \mathbf{k}$
34 that, by the continuity equation, do not couple to fluctuations in the charge density. Longitudinal
35 charge fluctuations can be probed by electron energy loss spectroscopy (EELS) but are limited
36 to energies above the Debye energy due to a phonon background (18, 19, 20). A classic method
37 to detect low frequency longitudinal charge dynamics is Mössbauer spectroscopy, successfully
38 used in the past to detect the slowing of the charge dynamics at charge ordering transitions of
39 Eu and Fe based compounds (21, 22).

40 However, the widespread adoption of Mössbauer methods has been long hindered by the
41 lack of suitable radioisotope sources. To overcome these difficulties, a new generation of
42 Mössbauer spectroscopy has recently been developed using synchrotron radiation (SR) (23).
43 SR-based Mössbauer spectroscopy (see Fig. 1 A) can be used for a wide range of Mössbauer

44 isotopes, providing improved energy resolution for these isotopes with shorter-lifetimes; it of-
45 fers an unprecedented capability to select a particular nuclear transition, taking advantage of
46 the perfectly polarized SR. This new approach presents an ideal probe to resolve *longitudinal*
47 charge dynamics in materials for which conventional Mössbauer techniques are inapplicable.

48 Here we report the first direct observation of critical charge dynamics in a SM regime using
49 SR-based ^{174}Yb Mössbauer spectroscopy. The heavy fermion metal $\beta\text{-YbAlB}_4$ provides an
50 ideal platform to study a SM regime at ambient pressure in a stoichiometric crystal (3, 24). In
51 $\beta\text{-YbAlB}_4$, core level X-ray studies have established the presence of an intermediate valence
52 state caused by valence fluctuations between two ionic configurations (25) $\text{Yb}^{2+} \rightleftharpoons \text{Yb}^{3+} + e^-$.
53 Usually, in heavy fermion compounds, such valence fluctuations are too fast to be observed by
54 Mössbauer spectroscopy (26, 27, 28, 29), but here we show that this is not the case in the SM.

55 Mössbauer spectroscopy measures the shift in a nuclear absorption line due to changes in
56 the local (q -integrated) charge density. The characteristic time-scale of the measurement is
57 the lifetime of the nuclear excited state, $\tau_0 \sim 2.5\text{ns}$ in ^{174}Yb . Charge fluctuations that are
58 much shorter in time than τ_0 produce a single motionally narrowed absorption line, whereas
59 charge fluctuations that are much longer in time than τ_0 produce a double peak absorption line,
60 corresponding to the two different valence states of the Yb ion (see Figure 1 C). By fitting
61 the Mössbauer absorption line-shape, one can detect charge fluctuations with time-scales in the
62 range $\sim 0.1\tau_0$ to $\sim 10\tau_0$ (30).

63 $\beta\text{-YbAlB}_4$ exhibits quantum criticality without tuning in an intermediate valence state (25),
64 and the application of an infinitesimal magnetic field B tunes the SM into a FL with $k_B T_{\text{FL}} \sim$
65 $\mu_B B$. The slope of the linear-in- T resistivity $\rho(T) \sim T$ over T between 0.5 and 25 K at
66 ambient pressure, corresponds to a nearly quantum-saturated scattering rate $\tau_{tr}^{-1} = 0.4 \times k_B T / \hbar$
67 (30), thus establishing $\beta\text{-YbAlB}_4$ as a system with Planckian dissipation (31). This anomalous
68 $\rho(T)$ and its extension over a broad pressure (p) range from ambient pressure to $p^* \sim 0.5\text{GPa}$

69 (3, 24, 32) (see Fig. 1 B) provides an excellent setting for high precision measurements of the
70 critical charge fluctuations, likely of relevance to the broader family of SMs.

71 We have investigated how the QC behavior in the SM regime affects the charge dynamics,
72 following their evolution as the SM regime at ambient pressure transforms into a FL regime
73 under pressure. Above 9K at ambient pressure (Fig. 2 A) the Mössbauer spectra exhibit a single
74 line feature. However, below $T^* \sim 10$ K, as one enters the QC region, this peak broadens into
75 a two-peak structure, with 5σ significance (30). Fig. 2 B shows how this two-peak structure
76 observed for $p < 0.7$ GPa at 2K coalesces into a single peak around $p \sim 1.2$ GPa, ultimately
77 sharpening into an almost resolution-limited peak at $p = 2.3$ GPa characteristic of a Fermi liquid
78 (30).

79 The local symmetry at the Yb site of β -YbAlB₄ with the orthorhombic structure allows us to
80 rule out a nuclear origin of the double-peak structure. For $c \parallel \mathbf{k}_0$ (the propagation vector of the
81 incident X-ray), the symmetry selects two degenerate nuclear transitions $I_g = 0 \rightarrow I_e^z = \pm 1$
82 from the five $E2$ nuclear transitions ($\Delta I^z = 0, \pm 1$, and ± 2) of the ¹⁷⁴Yb Mössbauer reso-
83 nance (33) (see Figs. 1 A and C). The absence of magnetic order in β -YbAlB₄ (24, 32) also
84 eliminates magnetic and non-axially symmetric quadrupolar hyperfine interactions as explana-
85 tions (30). This leaves a combination of the electric monopole and axially symmetric quadrupu-
86 lar interactions, linking the hyperfine energy to the valence state of the rare-earth ion, as the only
87 candidate for the observed splitting. The presence of a Mössbauer line splitting then implies
88 a distribution of Yb valences within the crystal. We now argue that these result from slow
89 dynamic charge fluctuations.

90 All Yb sites are crystallographically equivalent in β -YbAlB₄ and SR X-ray diffraction mea-
91 surements (34) show that the lattice structure does not change up to 3.5GPa at 7K; furthermore
92 the absence of any low-temperature phase transitions rules out the possibility of a charge den-
93 sity wave (30). Moreover, the residual resistivity ratio (RRR) exceeds 100, indicating the low

94 levels of quenched disorder in this material. Since disorder broadens the Mössbauer absorption
95 peak, our ability to resolve the double-peak structure is consistent with this conclusion.
96 An attempt to fit the Mössbauer spectrum with two nuclear transitions (i.e. a static hyperfine
97 interaction), using a width corresponding to the experimental energy resolution, fails to recon-
98 struct the feature at 2K and ~ 0 mm/s (blue broken line). Thus the two-peak structure and line
99 broadening observed for $T < 5$ K and $p < 0.7$ GPa must derive from a single nuclear transition
100 that is dynamically modulated by fluctuations between two different Yb charge states (i.e. a
101 time-dependent hyperfine interactions) (Fig. 1 C) (30).

102 We have analyzed our Mössbauer spectra at ambient pressure using a stochastic theory (35,
103 36, 37) with a single nuclear transition modulated by two different charge states (30). Fig. 2 A
104 shows that the predicted spectra (red lines) well reproduce the two-peak structure in the spectra
105 at low T s and its subsequent collapse into a single line with increasing T .

106 At ambient pressure, the extracted fluctuation time τ_f between two different Yb charge
107 states is unusually long compared to the electronic timescales, exhibiting a slow power-law
108 growth $T^{-\eta}$ ($\eta \sim 0.2$) on cooling below T^* (Fig. 2 C). The energy difference between two se-
109 lected nuclear transitions is almost independent of T up to 20K (30), so that the development of
110 the two-peak structure in the observed spectra must derive from the marked low- T growth in τ_f .
111 On the other hand, as shown in Fig. 2 B, the gradual collapse of the two-peak structure in the
112 observed 174 Yb Mössbauer spectra at 2K with increasing p indicates that fluctuation timescale
113 τ_f becomes shorter as a function of p . The spectra at $p < 1.2$ GPa can only be analyzed and
114 reconstructed by the same stochastic model used at the ambient pressure, while the spectrum
115 observed at 2.3GPa was simply fit using the static model. The line-width of this single ab-
116 sorption component was found to be $\Gamma = 1.11$ mm/s, slightly broader than the resolution limit
117 $\Gamma_0 = \hbar/\tau_0 = 1.00$ mm/s (3mK), for 174 Yb Mössbauer spectroscopy ($\tau_0 = 2.58$ ns).

118 As seen in Fig. 2 D, τ_f gradually decreases with increasing p , exhibiting a kink across $\sim p^*$

119 in between 0.5 and 1GPa, approaching the resolution limit at 2.3GPa. This is roughly consistent
120 with previous $\rho(T)$ measurements in β -YbAlB₄ (32); at $T < 0.5$ K and under p , $\rho(T)$ displays
121 $\rho \sim T^\alpha$ with $\alpha = 3/2$ below p^* and further application of pressure increases the exponent to
122 $\alpha = 2$, stabilizing a FL state at about 1GPa (32). However, the Fermi liquid temperature T_{FL}
123 depends on p , and only for $p \sim 2.3$ GPa is the system in the FL regime at $T = 2$ K (32).

124 The above consistency leads us to interpret the split line-shape observed in the Mössbauer
125 spectra of the SM as unusually slow valence fluctuations between the Yb²⁺ and Yb³⁺ ionic-like
126 states in β -YbAlB₄, on a timescale $\tau_f > 1$ ns that follows an approximate power-law growth
127 $\tau_f \sim T^{-0.2}$ with decreasing temperature below T^* . The Yb³⁺ ground state is a $J_z = \pm 5/2$
128 moment as deduced by varying incident angle of the X-ray (30). The slow charge fluctuations
129 extend up to p^* , beyond which a conventional valence fluctuation state with rapid charge fluc-
130 tuation takes over in the pressured regime corresponding to the FL regime.

131 The unusual aspect of the observed charge dynamics is that not only are they slower than the
132 Planckian time $\tau_f \gg \tau_{tr} \sim 10^{-2}$ ns at 2K, but they are also slower than the characteristic time-
133 scale of the lattice vibrations as we will show shortly. In this situation, the lattice is expected
134 to adiabatically respond to the associated charge redistribution. Each valence fluctuation of
135 Yb atoms is then dressed by N_p phonons, leading to the formation of a polaron (38, 39) and
136 renormalizing the matrix element for the charge fluctuations and providing a mechanism for
137 enhancing their time-scale ($\tau_f \rightarrow \tau_f e^{N_p}$) (30). Analysis of the Mössbauer spectra allows us
138 to directly check this scenario. We have used the T -dependence of the absorption components
139 in the spectra to determine the Lamb-Mössbauer (recoil-free) factor f_{LM} in β -YbAlB₄, the
140 equivalent of the Debye-Waller factor in a usual scattering experiment. Generally, $-\ln(f_{\text{LM}}) =$
141 $k_0^2 \langle \Delta z^2 \rangle$, where Δz is an atomic displacement from a regular position in a crystal along the

142 direction of \mathbf{k}_0 (40). The expression for the variance in atomic position is

$$\langle \Delta z^2 \rangle \propto \int_0^\infty d\omega \frac{F(\omega)}{\omega} \overbrace{\left[\frac{1}{2} + \frac{1}{e^{\omega/T} - 1} \right]}^{\frac{1}{2} \coth(\beta\omega/2)} \quad (1)$$

143 where $F(\omega)$ is the (partial) phonon density of states. In a Debye model, $F(\omega) \propto \omega^2$ which leads
 144 to $\langle \Delta z^2 \rangle \propto [3/2 + (\pi/\Theta_D)^2 T^2]$ at $T \ll \Theta_D$, where Θ_D is the Debye temperature (30). As
 145 seen in Fig. 3 A, this Debye relation holds above T^* at ambient pressure, where τ_f ($\sim 1.15\text{ns}$) is
 146 independent of T ; from this we estimate $\Theta_D = 95\text{K}$, corresponding to the lattice response time
 147 $\tau_L \sim h/k_B\Theta_D \sim 0.5\text{ps}$, so that $\tau_f \gg \tau_L$. The estimated Θ_D ($= 95\text{K}$) value is unusually smaller
 148 than that (195K) of a conventional valence fluctuation metal YbAl_2 (41). This indicates that
 149 the lattice vibrations are soft in $\beta\text{-YbAlB}_4$, suggesting an enhanced effective coupling between
 150 slow charge fluctuation modes and lattice vibrations.

151 Additionally, we see from Fig. 3A that in the QC regime below T^* , where τ_f develops
 152 temperature-dependence, $\langle \Delta z^2 \rangle$ departs from this Debye behavior, indicating an enhancement
 153 in the quantum fluctuations, $\langle \Delta z^2 \rangle = \langle \Delta z^2 \rangle_{\text{Debye}} + \delta\langle \Delta z^2 \rangle$, of the Yb ions. Notably, the
 154 $\sqrt{\delta\langle \Delta z^2 \rangle} \sim 0.014\text{\AA}$ rms fluctuation observed here is comparable to the quantum fluctuations
 155 of the phonon mode, around 0.05\AA estimated from $\frac{1}{4}k_B\Theta_D \sim \frac{1}{2}m_{\text{Yb}}(k_B\Theta_D/\hbar)^2\langle \Delta z^2 \rangle$. Fig. 3
 156 B shows that $\langle \Delta z^2 \rangle$ is approximately constant at 2K for $p < p^*$ and then drops when $p > p^*$,
 157 indicating that the anomalous vibrations of the lattice, $\delta\langle \Delta z^2 \rangle$, disappear in the FL regime at
 158 low temperatures.

159 The saturation of $\langle \Delta z^2 \rangle$ for $T < T^*$ and $p < p^*$ implies that the phonon spectrum $F(\omega)$
 160 has changed its form to compensate the $\coth(\beta\omega/2)$ term in the integral (1). This then sug-
 161 gests that at energies and temperatures below T^* , $F(\omega)$ acquires a temperature-dependence
 162 $F(\omega, T) = \phi(\omega) \tanh(\omega/2T)$ that cancels the $\coth(\omega/2T)$ term in integral (1). The function
 163 $\tanh(\omega/2T) \sim \omega/2T$ for $\omega \ll T$ and $\tanh(\omega/2T) \sim 1$ for $\omega \gg T$, and thus has the Marginal
 164 Fermi Liquid (MFL) form. This enhancement in phonon density of states should be observable

165 in inelastic neutron scattering measurements. Since the phonons are linearly coupled to the
166 charge density of the electrons, the appearance of a MFL component in the phonon spectrum is
167 an indication of MFL behavior in the charge fluctuations. The enhancement of τ_f by polaron
168 formation has been crucial for slowing the charge fluctuations down to time-scales accessible
169 to Mössbauer spectroscopy.

170 A possible interpretation of our results is the quantum critical tuning of a critical end point
171 of a classical valence transition (42) between the Yb^{2+} and Yb^{3+} ionic states. Such first order
172 valence transition lines, with second order end-points, are well established in rare earth com-
173 pounds. It has been suggested (42) that the tuning of such an endpoint to zero temperature may
174 provide an explanation of the observed Mössbauer spectra.

175 An alternative interpretation is that the observed valence fluctuation modes are an intrinsic
176 property of the SM regime connected with a spin charge separation that develops with the
177 collapse of the f -electron Fermi surface (43, 44, 45, 46). This scenario suggests that similar slow
178 charge fluctuations will be manifested in the Mössbauer spectra of any partial Mott localization
179 critical point, e.g. in other heavy-fermions and Iron-based superconductors.

180 In summary we have provided direct evidence for unusually slow charge fluctuations in the
181 SM regime of β - YbAlB_4 using a state-of-the-art technique, SR-based Mössbauer spectroscopy.
182 Because their time-scales are longer than that of the lattice response, we have inferred polaronic
183 formation in the mixed valence regime (38, 39). Both the slow charge fluctuation modes and the
184 anomalous vibrations of the lattice disappear in the pressure-induced FL regime. An interesting
185 possibility is that these observed slow charge modes are the origin of the linear resistivity often
186 observed in SMs. Various theoretical approaches (13, 14) have suggested that the novel transport
187 properties of SMs are linked to the universal quantum hydrodynamics of a Planckian metal.
188 Since the local equilibrium is established at the scale of Planckian time, it is natural to regard
189 the slow charge fluctuations detected here as a possible signature of a new hydrodynamic mode.

¹⁹⁰ This would lead us to expect that nano-second charge fluctuations and anomalous vibrations
¹⁹¹ are not unique to β -YbAlB₄, but rather, are universal properties of SM regimes in quantum
¹⁹² materials.

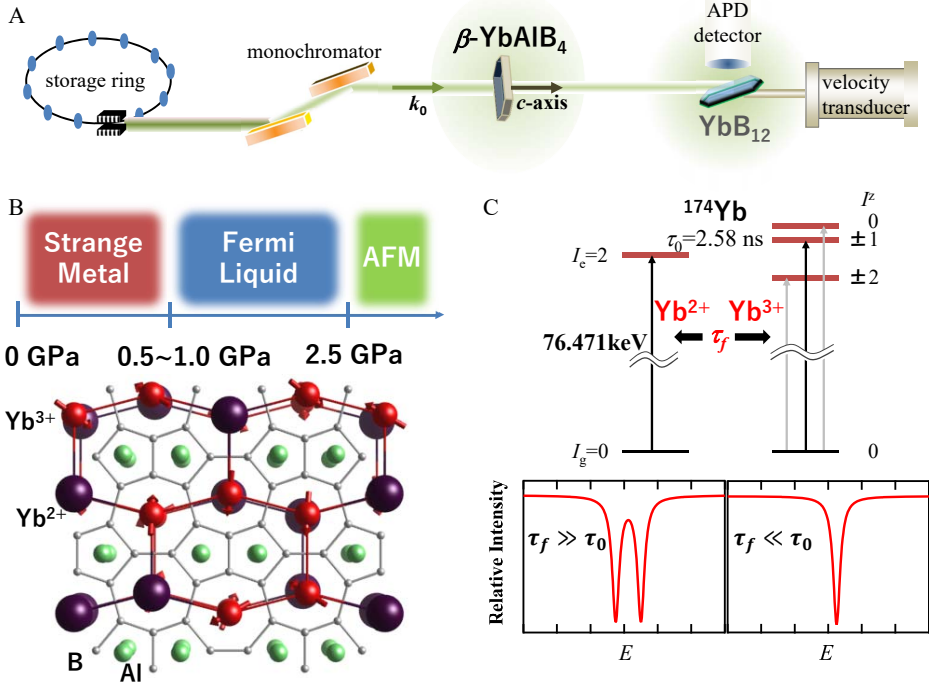


Figure 1: (A) Schematic of our experimental setup for the synchrotron-radiation-based ^{174}Yb Mössbauer spectroscopy (47). The ^{174}Yb nuclear resonance ($E_\gamma = 76.471\text{keV}$) was obtained by synchrotron radiation using a monochromator. The *c*-axis of the single crystalline β -YbAlB₄ samples was aligned along the propagation vector k_0 of the incident X-ray under both ambient and external pressure. The single-crystalline YbB₁₂ were cooled at 26K. A Si avalanche photodiode (APD) detector was used to measure delayed incoherent emission from ^{174}Yb nuclei in the YbB₁₂. (B) Schematic phase diagram of β -YbAlB₄ as a function of pressure at low temperatures (Top) and cartoon of the crystal structure of β -YbAlB₄ with a snapshot of the Yb valences, i.e., Yb²⁺ (large dark red sphere) and Yb³⁺ (small red sphere with arrow indicating magnetic moment) (Bottom). (C) (Top) Energy level diagrams of the excited ^{174}Yb ($I_e=2$) nuclear state with the lifetime of $\tau_0 = 2.58\text{ns}$ surrounded by different charge configurations. The allowed Mössbauer transitions are indicated by arrows, where the black arrows represent two selected transitions for $c \parallel k_0$. (Bottom) Two typical Mössbauer absorption spectra at limiting cases with $\tau_f \gg \tau_0$ and $\tau_f \ll \tau_0$ where τ_f is a characteristic timescale of fluctuation between two different charge configurations.

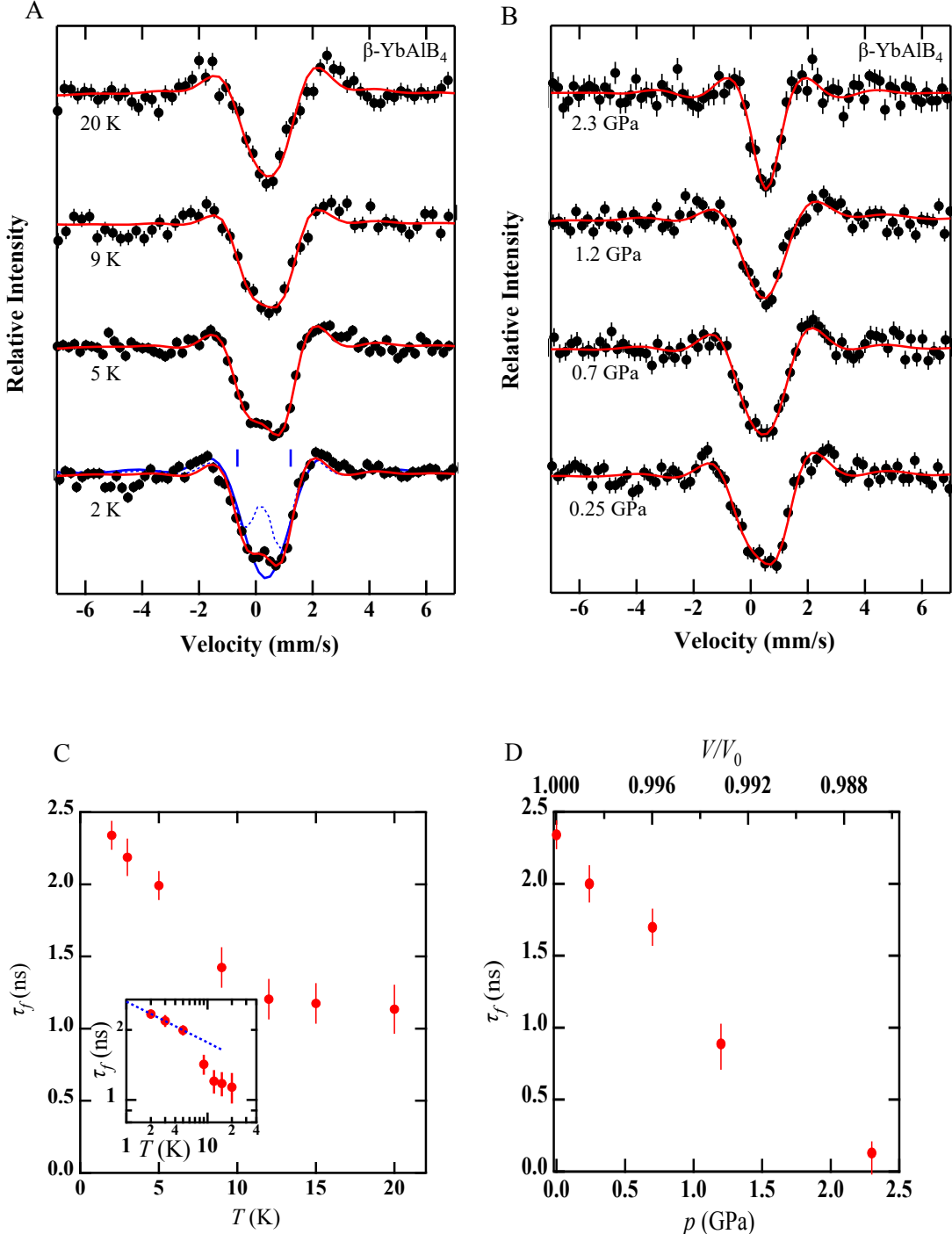


Figure 2: Selected synchrotron-radiation-based ^{174}Yb Mössbauer spectra of β -YbAlB₄ as a function of temperature (T) at ambient pressure (A) and under external pressure (p) at 2 K (B). The c -axis of the single crystalline β -YbAlB₄ samples was aligned along the propagation vector \mathbf{k}_0 of the incident X-ray. The solid circles with error bar and the red solid lines present the observed and the analytical spectra, respectively. In A, the broken blue line in the spectrum at 2 K represents the spectrum with two static nuclear transitions expected with our experimental energy resolution, whereas the solid blue line shows a fit to the wings of the lineshape, discarding the double-peak structure in the center. The deviation at the center corresponds to 5σ statistical significance (30). Temperature T (C) and pressure p (D) dependences of the refined fluctuation time τ_f between two different Yb charge states in β -YbAlB₄. (Inset in (C)) Log-log plots of τ_f versus T in β -YbAlB₄. The broken line represents $\tau_f \sim T^{-0.2}$.

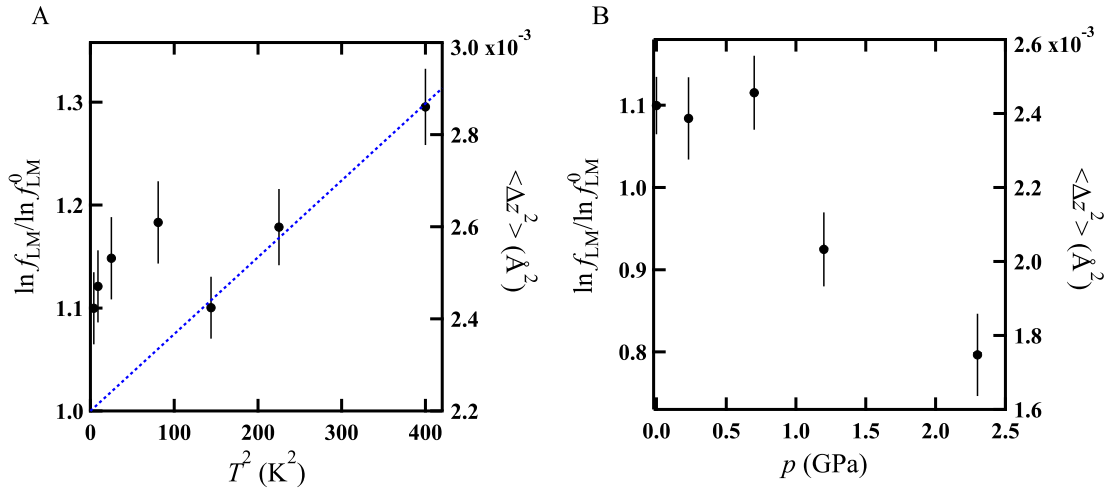


Figure 3: Lamb-Mössbauer factor f_{LM} ($\ln f_{\text{LM}} / \ln f_{\text{LM}}^0$) as a function of T^2 at ambient pressure (A) and under external pressure p at 2K (B) for β -YbAlB₄. In (A), the broken line represents a linear relation between $\ln f_{\text{LM}}$ and T^2 . In (A) and (B), $\ln f_{\text{LM}}^0 (\propto -\frac{3}{2} \frac{E_{\text{R}}}{k_{\text{B}} \Theta_{\text{D}}^{\text{Yb}}})$ was estimated above 12K at ambient pressure. For ¹⁷⁴Yb Mössbauer resonance of $k_0 = 38.75 \text{\AA}^{-1}$, $\langle \Delta z^2 \rangle$ for the Yb ions was evaluated in β -YbAlB₄ from the T and p dependences of $\ln f_{\text{LM}} / \ln f_{\text{LM}}^0$ using $\Theta_{\text{D}}^{\text{Yb}} = 95 \text{K}$. In (A) and (B), the $\langle \Delta z^2 \rangle$ values (right axis) are $\sim 2.6 \times 10^{-3} \text{\AA}^2$ in the SM regime and decrease to $1.7 \times 10^{-3} \text{\AA}^2$ in the pressured regime corresponding to the FL regime, which is comparable with that for YbAl₂ (41).

193 References and Notes

- 194 1. G. R. Stewart, *Rev. Mod. Phys.* **73**, 797 (2001).
- 195 2. T. R. Chien, Z. Z. Wang, N. P. Ong, *Phys. Rev. Lett.* **67**, 2088 (1991).
- 196 3. S. Nakatsuji, *et al.*, *Nature Physics* **4**, 603 (2008).
- 197 4. J. G. Analytis, *et al.*, *Nature Physics* **10**, 194 (2014).
- 198 5. S. Paschen, *et al.*, *Nature* **432**, 881 (2004).
- 199 6. H. Shishido, R. Settai, H. Harima, Y. Ōnuki, *J. Phys. Soc. Jpn.* **74**, 1103 (2005).
- 200 7. P. Gegenwart, Q. Si, F. Steglich, *Nature Phys.* **4**, 186 (2008).
- 201 8. K. Kuga, *et al.*, *Sci. Adv.* **4**, eaao3547 (2018).
- 202 9. F. Laliberté, *et al.*, *Nature Communications* **2**, 432 (2011).
- 203 10. E. Fradkin, S. A. Kivelson, M. J. Lawler, J. P. Eisenstein, A. P. Mackenzie, *Annual Review*
204 *of Condensed Matter Physics* **1**, 153 (2010).
- 205 11. J.-H. Chu, *et al.*, *Science* **329**, 824 (2010).
- 206 12. M. Lawler, *et al.*, *Nature* **466**, 347,351 (2010).
- 207 13. J. Zaanen, Y.-W. Sun, Y. Liu, K. Schalm, *Holographic Duality in Condensed Matter Physics*
208 (Cambridge University Press, 2016).
- 209 14. S. A. Hartnoll, A. Lucas, S. Sachdev, *Holographic Quantum Matter* (MIT Press, 2018).
- 210 15. S. A. Hartnoll, A. P. Mackenzie, *ArXiv:2107.07802* (2021).
- 211 16. P. T. Brown, *et al.*, *Science* **363**, 379 (2019).

²¹² 17. L. Prochaska, *et al.*, *arxiv: 1808.02296 (2018)*. (2018).

²¹³ 18. S. Vig, *et al.*, *SciPost* **3**, 026 (2017).

²¹⁴ 19. M. Mitrano, *et al.*, *Proc Natl Acad Sci USA* **115**, 5392 (2018).

²¹⁵ 20. A. A. Husain, *et al.*, *Physical Review X* **9**, 041062 (2019).

²¹⁶ 21. O. Berkooz, M. Malamud, S. Shtrikman, *Solid State Communications* **6**, 185 (1968).

²¹⁷ 22. M. Takano, N. Nakanishi, Y. Takeda, S. Naka, *J. Phys. Colloques* **40**, C2 (1979).

²¹⁸ 23. M. Seto, *et al.*, *Phys. Rev. Lett.* **102**, 217602 (2009).

²¹⁹ 24. Y. Matsumoto, *et al.*, *Science* **331**, 316 (2011).

²²⁰ 25. M. Okawa, *et al.*, *Phys. Rev. Lett.* **104**, 247201 (2010).

²²¹ 26. C. M. Varma, *Rev. Mod. Phys.* **48**, 219 (1976).

²²² 27. E. V. Sampathkumaran, *Hyperfine Interactions* **27**, 183 (1986).

²²³ 28. R. L. Cohen, M. Eibschütz, K. W. West, *Phys. Rev. Lett.* **24**, 383 (1970).

²²⁴ 29. I. Nowik, *Hyperfine interactions* **13**, 89 (1983).

²²⁵ 30. *Supplementary material is available on Science online* .

²²⁶ 31. A. Legros, *et al.*, *Nature Physics* **15**, 142 (2019).

²²⁷ 32. T. Tomita, K. Kuga, Y. Uwatoko, P. Coleman, S. Nakatsuji, *Science* **349**, 506 (2015).

²²⁸ 33. J. P. Hannon, G. T. Trammell, M. Blume, D. Gibbs, *Phys. Rev. Lett.* **61**, 1245 (1988).

²²⁹ 34. Y. Sakaguchi, *et al.*, *J. Phys. Soc. Jpn.* **85**, 023602 (2016).

²³⁰ 35. P. W. Anderson, *J. Phys. Soc. Japan* **9**, 316 (1954).

²³¹ 36. R. Kubo, *J. Phys. Soc. Japan* **9**, 935 (1954).

²³² 37. M. Blume, *Phys. Rev.* **174**, 351 (1968).

²³³ 38. D. Sherrington, P. Riseborough, *J. Phys. Colloques* **37**, C4 (1976).

²³⁴ 39. A. C. Hewson, D. M. Newns, *Journal of Physics C: Solid State Physics* **12**, 1665 (1979).

²³⁵ 40. G. T. Trammell, *Phys. Rev.* **126**, 1045 (1962).

²³⁶ 41. D. Weschenfelder, *et al.*, *Hyperfine Interactions* **16**, 743 (1983).

²³⁷ 42. S. Watanabe, K. Miyake, *Phys. Rev. Lett.* **105**, 186403 (2010).

²³⁸ 43. M. Oshikawa, *Phys. Rev. Lett.* **84**, 3370 (2000).

²³⁹ 44. T. Senthil, S. Sachdev, M. Vojta, *Phys. Rev. Lett.* **90**, 216403 (2003).

²⁴⁰ 45. J. H. Pixley, S. Kirchner, K. Ingersent, Q. Si, *Phys. Rev. Lett.* **109**, 086403 (2012).

²⁴¹ 46. Y. Komijani, P. Coleman, *Phys. Rev. Lett.* **122**, 217001 (2019).

²⁴² 47. R. Masuda, *et al.*, *Appl. Phys. Lett.* **104**, 082411 (2014).

²⁴³ We would like to thank M. Takigawa for very useful discussions and F. Iga for preparation
²⁴⁴ of single-crystalline YbB_{12} . The SR-based ^{174}Yb Mössbauer experiments were performed at
²⁴⁵ BL09XU and BL19LXU on SPring-8 with the approval of the Japan Synchrotron Radiation
²⁴⁶ Research Institute (JASRI) (Proposal Nos. 2011A1450, 2012B1521, 2013B1393, 2015A1458,
²⁴⁷ 2016A1363, and 2019B1597) and RIKEN (Proposal Nos. 2016110, 20170019, 20180019, and
²⁴⁸ 20190025). This work is partially supported by Grants-in-Aids for Scientific Research on In-
²⁴⁹ novative Areas (15H05882 and 15H05883) from the Ministry of Education, Culture, Sports,

250 Science, and Technology of Japan, by CREST (JPMJCR18T3), Japan Science and Technol-
251 ogy Agency, and by Grants-in-Aid for Scientific Research (15K05182, 16H02209, 16H06345,
252 19H00650, and 23102723) from the Japanese Society for the Promotion of Science (JSPS), by
253 the Canadian Institute for Advanced Research, the National Science Foundation grant DMR-
254 1830707 (P. Coleman and Y. K) and by the U. S. Department of Energy (DOE), Office of
255 Science, Basic Energy Sciences under award DE-SC0020353 (P. Chandra). The Institute for
256 Quantum Matter, an Energy Frontier Research Center was funded by DOE, Office of Science,
257 Basic Energy Sciences under Award # DE-SC0019331. P. Chandra and P. Coleman thank S.
258 Nakatsuji and the Institute for Solid State Physics (Tokyo) for hospitality when early stages of
259 this work were underway. P.C., P.C. and Y.K. acknowledge the Aspen Center for Physics and
260 NSF Grant No. PHY-1607611 where this work was discussed and further developed.